HarmFlo+ Tech Notes

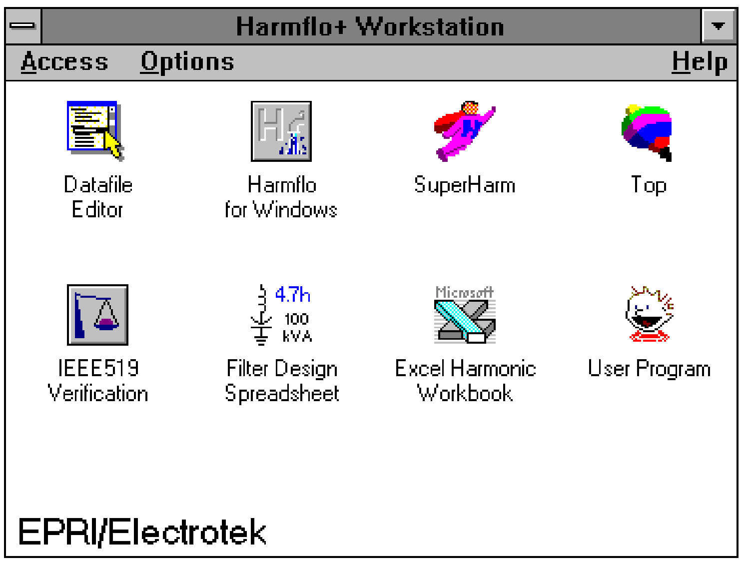

for users of the EPRI/Electrotek HarmFlo+ Workstation

Issue # 95-1 ***May, 1995*** ***Editor: Susie Brockman***

Project Manager: Tom Grebe

in this issue:

Letter from the Editor:

This is the fifth issue of *HarmFlo+ Tech Notes*. The technical newsletter provided to members of the HarmFlo User's Group. It was developed as a technical bulletin for exchanging information between members of the group. We are constantly seeking new information to share. Following is a list of the types of articles you may want to submit.

- Technical articles
- Modifications / enhancements to the code
- Case studies / unique simulations
- Research projects
- SuperHarm / HARMFLO data preparation / model development
- Include / library files developed for distribution on the BBS
- Letters to the editor / User's Group
- Technical paper abstracts
- Questions for members of the User's Group

If you feel you have an article which is appropriate, or may help another member of the group with harmonic analysis, please send us a copy for review. We feel the exchange of information is one of the most helpful resources the group can provide.

Sincerely,

For more information concerning the newsletter or to submit a contribution please contact:

Susie Brockman
Electrotek Concepts, Inc.
408 North Cedar Bluff Road, Suite 500
Knoxville, Tennessee 37923
Phone: (615) 470-9222 x41 FAX: (615) 470-9223
e-mail: susieb@electrotek.com

SuperHarm Advanced Models

MACHINE

The MACHINE model is used to represent a generator or motor as a frequency dependent branch. The model alone can represent a motor. The branch impedance at fundamental frequency is calculated as follows:

$$R_1 = \frac{100 \cdot Z_b}{\% Load}, \quad X_1 = R_1 * Tan\left(Cos^{-1} \frac{\% PF}{100}\right)$$

Resistance and reactance at harmonic frequencies is given by %Rh and %Xh, respectively. Subtransient resistance and reactance are usually used for these parameters. By default, losses are frequency-dependent; the program assumes that resistance, as well as reactance, increases linearly with frequency. Resistance and reactance should be entered in percent on the impedance base corresponding to the terminal voltage, horsepower, and efficiency:

$$Z_b = \frac{kV_b^{\,2}}{MVA_b} = \left(\frac{13.412 * \%Eff}{HP}\right) \cdot kV^2$$

%Rh and %Xh are optional. The default values correspond to:

$$X_h = 0.170 * X_1$$
$$R_h = 0.025 * X_h$$

To model a generator it is necessary to use the VSOURCE model behind the MACHINE model to represent the 60Hz voltage source. This is necessary to obtain the correct power flow generated between the generator and the system. It should be noted that it may be necessary to vary the voltage and differential angles to obtain the most accurate representation of the generator. This voltage is usually larger then 1.0 per unit on the machines base.

LINE

LINE can be used to represent any number of mutually-coupled, multi-phase transmission lines. Phase unbalance, skin effect, and the frequency dependence of the earth return path (Carson's equations) are included in the model. LINE requires detailed information concerning conductor characteristics and tower geometry. The conductor data for the LINE model is entered in a series of lists. Each list contains the data for all the conductors of the type indicated by the list tag name.

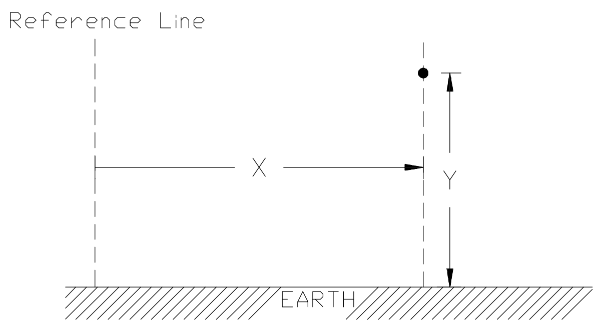

The LINE model can also be used to generate an output listing of the calculated line constants. A sample line constants output can be seen below:

```
Number of Phase  Conductors ...: 3
Number of Ground Conductors ...: 0
Frequency for Constants (Hz) ..: 60
Earth Restivity (ohm-meters) ..: 100
Units for Input Data ..........: English
ID    DC Res.   GMR    Diameter     X Coord     Y Coord  NB   Spacing
      ohms/mi   feet    inches        feet        feet         inches
--   ---------  ----  ----------  ----------  ---------- --    ------
 P  0.062137  0.0125      0.025         -15          15   1       0
 P  0.062137  0.0125      0.025           0          15   1       0
 P  0.062137  0.0125      0.025          15          15   1       0
L mH/km - Before reduction:
 2.4651        1.0471        0.90844
..
Z Ohms/km - Before ground wire reduction:
 0.097585      0.058528      0.058517
 0.92931       0.39473       0.34247
..
Z Ohms/km - After  ground wire reduction:
 0.097585      0.058528      0.058517
 0.92931       0.39473       0.34247
..
C nF/km:
```

```
 5.4557       -0.41569      -0.15156
..
YC micro Siemens/km:
 2.0567       -0.15671      -0.057138
..
Attenuation Alpha - micro Nepers/km:
 111.14
..
Characteristic Impedance Zc - Ohms:
 965.96
-61.219
..
Characteristic Impedance Zc (Polar) - Ohms:
 967.90
-3.6263
..
Velocity - km/s:
 2.1536E+05
..
```

INDUCTIONMOTOR

INDUCTIONMOTOR models a single-phase or three-phase induction motor. Besides the device name and bus names, only rated power (HP) and terminal voltage (kV, line-neutral for the single-phase model, line-line for the three-phase model) must be entered. The remaining parameters default to specific values indicated in the SuperHarm manual. The model parameters and assumptions utilized in SuperHarm are based upon a paper titled “Studies on Modeling Harmonic Impedance for Induction Motors” by Zhang Jing and He Fengreng.

Four assumptions are made for this model:

- Stator impedance is equal to that of the rotor
  $x_1 = x_2$.
- Exciting impedance is 35 times as high as that of stator
  $x_m = 35x_1$
- Exciting current is 30% of stator current. The remaining 70% of stator current flows through the rotor circuit, i.e., $I_0 = 30\% \, I_1$ and $I_2 = 70\% \, I_1$.
- Core loss of induction motor takes 3% that of the total power output.

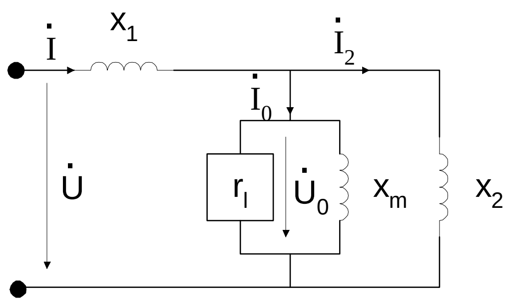

For the above figure, the reactive power equation is listed as follows:

$$Q_m/3 = I^2 x_1 + I_2^2 x_2 + I_0^2 x_m$$

Substituting with the assumptions made above the following results:

$$x_1 = (Q_m U^2) / 4.64 (P_m^2 + Q_m^2)$$

core resistance is as follows:

$r_l = (U_o^2) / 0.03 P_m \eta$, where η is the efficiency of the motor
Rotor slip, S, is computed from the number of stator pole pairs and the operating shaft speed.

$$S = 1 - \frac{RPM \cdot Poles}{120 \cdot f}$$

where *f* is the fundamental frequency.

CMATRIX

CMATRIX simply allows the user to enter the capacitances for a system in a matrix formation. The diagonal values in the matrix are assumed to be shunt connected. The purpose of this option is to allow ease in the representation of multi-phase capacitance.

ZYCMATRIX

ZYCMATRIX allows representation of any number of mutually coupled branches. Branch self and mutual impedances are entered as R (ZRMATRIX) and X (ZXMATRIX) matrices, where:

`rii`, `xii` are the resistance and inductive reactance of branch i,
`rij`, `xij` are the real and reactive components of the coupling impedance from branch i to branch j.

Reactance values should be entered at fundamental frequency. They may be inductive (X > 0) or capacitive (X < 0). All components of the [R] matrix, on the other hand, must be non-negative. Zero values are acceptable for coupling impedances, but not for self impedances. That is, for branches i and j, r_{ij}, x_{ij} may both be zero; but r_{ii} and x_{ii} cannot both be zero.

The admittance values are entered using YCMATRIX, where:

yii the admittance of branch i,
yij the admittance from branch i to branch j.

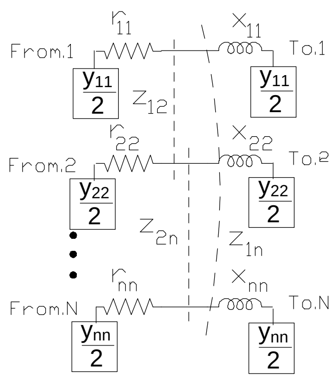

Afroz K. Khan,
Power Systems Engineer
Electrotek Concepts, Inc.

Case Study

A Harmonic Sensitivity Study Involving Variable Speed Heat Pumps

Introduction

Proper power quality assessment procedures are not only essential when developing solutions for existing distortion problems, but also when computer simulations are used to quantify potential distortion levels due to the insertion of nonlinear loads in a distribution system under study. Consistent with the recommendations and general procedures outlined in [1], harmonic distortion was identified as the major power quality concern with emphasis on voltage distortion caused by variable-speed heat pumps (VSHPs).

Initially, the distribution system must be accurately modeled for preliminary simulations using harmonic simulation tools or computer programs; this is normally done through the accumulation of system data followed by the development of *appropriate* models for each system component. Once the distribution system has been characterized in sufficient detail, preliminary simulations can then be performed to determine the system resonant frequencies; that is, to quantify the impedance characteristics of the distribution system as a function of frequency.

This paper presents the simulation results of a harmonic sensitivity study performed on the C433 feeder of Figure 1 which investigates the effect of feeder capacitor configuration and size, as well as the effect of system damping on propagating harmonic currents. The motivation for this paper came from preliminary computer simulation results which showed evidence of anomalous behavior which could only be explained by possible resonance conditions existing on Circuit C433. It is well known that the response of a distribution system is governed by the interaction of the system inductance and capacitance in addition to the resistive damping provided by the system loads and component losses.

Preliminary Information

The substation and feeder capacitor sizes and locations play an important role in the operation of the distribution system. The impedance of a capacitor, $Z_C = -j/wC$ (Ω), is inversely proportional to the capacitor size, C (μF), and the system frequency, (in radians per second).

Figure 1 One-line diagram of the distribution system.

Clearly as *w* increase, Z_C approaches a short circuit, and a shunt path to ground is created for the harmonic currents.

The installation of power factor correction capacitors may result in resonance conditions at harmonic frequencies. These undesirable conditions can usually be avoided by changing the location and/or size of the bank or detuning the bank with a series reactor at the resonant frequency. In effect, the resulting LC filter located in parallel with the harmonic source becomes a low-impedance path to ground and little harmonic current flow into the AC system is achieved.

A parallel resonant frequency, as seen looking back into the distribution system from any bus along the feeder, can quickly be estimated using the simple formula

(1)

where *h* is the harmonic order, $X_{C,1}$ and $X_{TH,1}$ are the equivalent capacitance of the shunt compensation and the Thévenin inductive reactance at the fundamental frequency for the bus of interest [2].

A parallel resonance occurs when the inductive and capacitive reactance as seen from the bus cancel; that is, when $X_C = X_{TH}$, the impedance is a maximum (ideally infinite), and the resulting harmonic voltage at bus *i* due to the harmonic injection at bus *j* is a maximum. This condition is typically termed an overvoltage. In the case of a series resonance, the converse is true; that is, the Thévenin inductive reactance is in series with the equivalent capacitance. This implies that when $X_C = X_{TH}$, the impedance is a minimum (ideally zero), and the current is a maximum. This condition is typically termed current magnification.

Before presenting the frequency response characteristics obtained for Circuit C433, it is necessary to discuss the following two terms used in impedance classification — driving point and transfer quantities. The former (i.e., Z_{i-i}^h) relates the *h*th harmonic current injected at the *i*th bus (i.e., I_i^h) to the resulting *h*th harmonic voltage response at the *i*th bus (i.e., V_i^h) when *all other current injections* are open circuited. The transfer impedance (i.e., Z_{i-j}^h) relates the *h*th harmonic current injected at the *j*th bus (i.e., I_j^h) to the resulting *h*th harmonic voltage response at the *i*th bus (i.e., V_i^h) when *all other current injections* are open circuited.

The driving-point and transfer impedances may then be divided into three additional classes: positive-, negative-, and zero-sequence impedances. These so-called sequences are derived from Fortescue's method of symmetrical components which transforms an *unbalanced N*-phase set of voltages or currents (i.e., *abc* variables) to *N balanced sets* of components by the transformation matrix

(2)

where a = 1∠120 and the triple of phase currents, I_{abc}, is shown below:

(3)

If one considers the triplet of balanced three-phase currents with *h* = 1, and a,1, b,1, and c,1 having the values of 0 , -120 , and 120 , then the respective current phasors form a positive- or *abc*-sequence set. Similarly, for *h*=*n*, the three-phase current phasors determine either a positive-, negative-, or zero-sequence set. For example, with *h* = 2, the phase angles of the three currents become: 0 , -240 , and 240 ; this is a negative- or *acb*-sequence. When *h* = 3, the phase angles are: 0 , -360 , and 360 , a zero-sequence set since all currents are in phase. Table I summarizes the relationship which exists between the harmonic order, *h*, of a three-phase set of currents or voltages and its associated sequence network. In general, harmonic orders, *h*, of *3k*, *3k+1*, and *3k-1* correspond to the zero, positive, and negative sequence, respectively, for non-negative integers *k* and *h*.

The importance of the symmetrical component transformation is that the three sequences are decoupled; that is, the positive-, negative-, and zero-sequence networks can be solved separately using single-phase analysis and then transformed back to the phase variables.

Table I The associated sequence network as a function of harmonic order, *h*.

Harmonic order, h	*Associated sequence network*
1	positive
2	negative
3	zero
4	positive
5	negative
6	zero
7	positive
8	negative
9	zero
10	positive

The following statements of Ohm's law are then valid:

(4)

where the subscripts +, -, and *0* denote the positive-, negative-, and zero-sequence quantities. Thus, the product of a positive-sequence current and impedance can only result in a positive-sequence voltage; the same is true for the negative- and zero- sequence networks. As in this study when only balanced conditions are considered, the positive- and negative-sequence impedances are identical, i.e., $Z_+^h = Z_-^h$.

Driving-Point Impedance Results

Figure 2 displays the magnitude of the positive-sequence, driving-point impedances at buses 5 and 6 of Circuit C433 with the 600-kVAr switched capacitors connected at buses 5 and 6. The magnitude of the driving-point impedance at bus 5 shows parallel resonances at the fifth (≅350%), eighth (≅270%), and 32nd harmonics. A series resonance also exists at the 20th harmonic. The parallel resonances existing at bus 6 are at the fifth (≅410%) and eighth (≅390%) harmonics with lesser resonance peaks at the 22nd (≅180%) and 32nd (≅250%) harmonics. Since the system in Figure 1 is assumed to be balanced, the positive- and negative-sequence networks are identical. Thus, positive- and negative-sequence currents injected at buses 5 and 6 interact with $\boldsymbol{Z}_{5,5}$ and $\boldsymbol{Z}_{6,6}$ to produce harmonic voltages via (4).

Figure 2 - Positive-sequence driving-point impedances at buses 5 and 6 of Circuit C433 with the switched-capacitor banks connected.

Figure 3 depicts the magnitude of the zero-sequence driving-point impedances at buses 5 and 6 of Circuit C433 with the 600-kVAr switched capacitors connected at buses 5 and 6. The harmonic order of the dominant parallel resonant frequencies at bus 5 are the fourth (≅480%) and the 17th (≅ 930%); a series resonance exists at the 11th harmonic. The harmonic orders of the existing parallel resonances at bus 6 are: the fourth (≅600%), the 11th (≅180%), and at the 17th (≅550%). Note that the impedances shown in Figure 3 determine the voltage responses to zero-sequence currents injected at buses 5 and 6, respectively. Although a parallel resonance occurs at 240 Hz, a nearly equal third-harmonic impedance magnitude exists which may result in a substantial third-harmonic voltage drop.

Figures 4 and 5 depict the magnitude of the positive- and zero-sequence driving-point impedances at buses 5 and 6 of Circuit C433 when the 600-kVAr switched capacitors at buses 5 and 6 are disconnected. Comparing Figures 2 and 4, the lower-order resonant frequencies have shifted from the fifth and eighth to the sixth and eleventh harmonics, respectively. This shift in resonance to a higher frequency is expected since the equivalent capacitance at buses 5 and 6 has substantially decreased; thus by (1), the harmonic order, h, must increase. It should be noted that the resonant frequency at the 32nd harmonic has been replaced by a parallel resonance at the 17th harmonic.

Figures 3 and 5 show drastic changes in the zero-sequence driving-point impedance characteristic at buses 5 and 6. Note that at frequencies higher than the 11th, the system looks almost completely inductive (i.e., $Z_{TH} \cong h w L_{TH}$). A substantial resonant peak at the ninth harmonic now exists.

Figure 3 - Zero-sequence driving-point impedances at buses 5 and 6 of Circuit C433 with the switched-capacitor banks connected.

Figure 4 -Positive-sequence driving-point impedances at buses 5 and 6 of Circuit C433 with the switched-capacitor banks disconnected.

Figure 5 - Zero-sequence driving-point impedances at buses 5 and 6 of Circuit C433 with the switched-capacitor banks disconnected.

The significance of the positive- and zero-sequence driving-point impedances at buses 5 and 6 are independent of the *single* current injection in Circuit C433 (i.e., at bus 55) shown in Figure 1. In fact, these impedances usually become significant when a harmonic source is located at either one or both of these buses or when a harmonic penetration study is being performed.

Transfer Impedance Results

Figures 6 and 7 show the magnitude of the positive- and zero-sequence transfer impedances between bus 55 and buses 5 and 6 of Circuit C433 with the 600-kVAr switched capacitors connected at buses 5 and 6.

Figure 6 - Positive-sequence transfer impedances between bus 55 and buses 5 and 6 of Circuit C433 with switched-capacitor banks connected.

Figure 7 - Zero-sequence transfer impedances between bus 55 and buses 5 and 6 of Circuit C433 with switched-capacitor banks connected.

Figure 6 shows that both transfer impedance magnitudes behave quite similarly since they are located electrically close to each other in the system. A substantial fifth-harmonic resonance exists for $\boldsymbol{Z}_{5,55}$ (≅ 350%) and $\boldsymbol{Z}_{6,55}$ (≅370%), respectively. The other resonance peaks appear at the eighth and 31st harmonic orders. Note that a positive- *or* negative-sequence current with significant energy can excite one of the modes of the system. The high-frequency resonant frequency is not of much concern since negligible harmonic components exist at this frequency for the injection at bus 55. This can be verified by observing the harmonic spectra of the VSHPs. The resonant peak at the eighth harmonic is insignificant since there is no current harmonic component to interact with at this frequency. The only resonant frequency of concern should be the fifth harmonic; this is true since a significant voltage response may result due to the fifth-harmonic current injection at bus 55.

Figure 7 displays resonances at the ninth (≅235%) and 17th (≅325%) harmonics. Although it may seem that only one trace exists, the impedance magnitudes versus the harmonic order are virtually identical. Since the ninth-harmonic current injection at bus 55 is non-negligible, a significant ninth-harmonic voltage may develop at buses 5 *and* 6.

Figures 8 and 9 display the magnitude of the positive- and zero-sequence transfer impedances between bus 55 and buses 5 and 6 of Circuit C433 with switched-capacitor banks disconnected. Once again, in both figures it appears as if a single trace exists; this is not the case but the results are virtually indistinguishable from each other. Figure 8, of concern when investigating positive- or negative-sequence currents injected at bus 55, shows resonance phenomena at the sixth (≅150%), 11th (≅200%), and 17th (≅520%) harmonics. Relative to Figure 6, one would not expect as much voltage distortion due to the fifth-harmonic current injection at bus 55 with this transfer characteristic.

Figure 8 - Positive-sequence transfer impedances between bus 55 and buses 5 and 6 of Circuit C433 with switched-capacitor banks disconnected.

Figure 9 - Zero-sequence transfer impedances between bus 55 and buses 5 and 6 of Circuit C433 with switched-capacitor banks disconnected.

Comparing Figures 7 and 9, one notes that the resonance at the 17th harmonic has vanished with the switched capacitor disconnected from the system and that the impedance magnitude at the ninth harmonic has increased by approximately three. Since the ninth-harmonic current magnitude of the injection at bus 55 is approximately 4%, a small voltage THD results.

Figures 2 to 9 have been used to characterize the system response as a function of frequency. Although Figures 2 to 5 do not deal directly with a harmonic study considering a single current injection at buses other than 5 or 6, they are extremely helpful in understanding the mechanisms by which voltage total harmonic distortion is generated when performing a harmonic penetration study. Realizing that Figures 6 to 9 are of most importance, it is now possible to discuss the harmonic sensitivity of the system to changes in the switched-capacitor sizes at buses 5 and 6.

Voltage Distortion Sensitivity to Feeder Capacitor Configuration and Size

Table 2 provides important information regarding the sensitivity of each capacitor bank on Circuit C433 of DS1 in Figure 1. For this sensitivity study, the low-loading condition was used throughout with a maximum number of VSHPs (i.e., 11) connected to the 50-kVA distribution transformer between buses 5 and 55. The figure of merit (FOM) chosen to express the sensitivity of each capacitor configuration is the arithmetic mean of all voltage THDs along Circuit C433; that is, buses 1-8, and bus 55 in Figure 1. Mathematically, the figure of merit may be expressed by the following relationship:

(5)

The "base case" capacitor configuration — Case 8 in Table 2 — used throughout this study consisted of a 600-kVAr fixed capacitor at bus 2 and 600-kVAr switched capacitors at buses 5 and 6 in Figure 1; this configuration resulted in the maximum voltage total harmonic distortion on the feeder. This result is contrary to that expected since the capacitors *should* act as sinks to the harmonic currents thus diminishing the distortion levels along the feeder; the significance of this phenomenon will be discussed shortly. From Table 3.2, the following observations may be made:

- All capacitor configurations amplify the injected harmonic currents at bus 55 and thus increase the voltage distortion along the feeder.

- As the figure of merit increases in Table 2, the voltage total harmonic distortion sensitivity increases for the fixed-current injection at bus 55. Thus, as the figure of merit increases, the less desirable is the feeder capacitor configuration.

- The capacitor at bus 6 is more sensitive to the harmonic injection at bus 55 than the capacitor at bus 5.

- The harmonic sensitivity when the capacitors at buses 5 and 6 are connected to the distribution feeder is noticeably increased over that when buses 2 and 5 or buses 2 and 6 have connected capacitor banks.

Table 2-The eight possible configurations for the capacitors at buses 2, 5, and 6 and their respective figures of merit.

Case	*Bus 2 Capacitor (kVAr)*	*Bus 5 Capacitor (kVAr)*	*Bus 6 Capacitor (kVAr)*	*FOM*
1	0	0	0	0.700
2	600	0	0	0.750
3	0	600	0	0.895
4	0	0	600	0.922
5	600	600	0	0.964
6	600	0	600	1.007
7	0	600	600	1.377
8	600	600	600	1.530

From the above observations, it is clear that some kind of anomalous behavior exists at buses 5 and 6. As alluded to earlier, the presence of power factor correcting capacitors typically act as a *harmonic sink*. This implies that as the radian frequency increases, the impedance of the capacitor decreases, and the harmonic currents encounter a relatively smaller shunt impedance path to ground. The capacitor is then said to "sink" the harmonic currents. When this expected behavior is not observed, it is suspected that a resonance condition may exist.

Harmonic Sensitivity Due to the Capacitor Size

The eight capacitor configurations shown in Table 2 provided information on which capacitor banks were most sensitive to the single current harmonic injection at bus 55. In order to understand how the capacitor size relates to this sensitivity, the fixed capacitor at bus 2 was held constant at 600 kVAr while the banks at buses 5 and 6 were varied in 300 kVAr increments. The results of this exercise are summarized in Table 3.

It may be quite surprising to see such a large variance among the figure of merit — from 0.98 to 1.963 — for the 16 different cases simulated in Table 3. Clearly, many more sizing arrangements exist; however, since the capacitors are installed in the field in 300 kVAr increments, the results of Table 3 represent realistic operating points for the system under study. In general, the complexity of even a small system like that depicted in Figure 1 precludes an analysis without the use of a digital computer. The result of this investigation shows that the worst-case voltage distortion scenario results when the switched capacitors at buses 5 and 6 have the values 1200 and 600 kVAr, respectively.

Voltage Distortion Sensitivity To System Damping

The response of the distribution system is governed by the interaction of the system inductance and capacitance in addition to the resistive damping provided by loads and other system component losses. System damping is due mainly to the leakage reactance of transformers, line losses, and system loading. To this end, computer simulations were performed to demonstrate how one can *qualitatively* determine the effects of system damping on the resulting voltage total harmonic distortion along the C433 feeder.

Table 4 shows the resulting feeder harmonic distortions and corresponding figures of merit for the following deviations from the base case: *(a)* doubling the line length of Circuit C433, *(b)* no linear load at bus 55, *(c)* the linear load is removed from Circuit C433 (i.e., low-loading levels used for the base case remain connected to the buses on the other three feeders), and *(d)* linear load is completely removed from DS1. The results presented in Table 4 for doubling the feeder length show little variation from the base case. Specifically, if every impedance in the network is doubled, the transfer impedances between bus 55 and all other buses must double, and for a fixed-harmonic current injection at a single bus, the voltage fundamental and harmonic components at all buses must also double. However, this is not the case since *only the line impedances have been doubled* — not the distribution or power transformer impedances. Therefore, it is not clear what effect this action has on the FOM.

Table 3 The effect of capacitor bank size on the resulting voltage total harmonic distortion.

Bus 2 Cap (kVAr)	*Bus 5 Cap (kVAr)*	*Bus 6 Cap (kVAr)*	*Bus 1*	*Bus 5*	*Bus 6*	*Bus 55*	*Bus 8*	*FOM*
600	300	300	0.46	1.21	1.25	2.80	1.25	**0.980**
600	300	600	0.59	1.54	1.65	3.09	1.65	**1.224**
600	300	900	0.78	2.06	2.29	3.45	2.29	**1.592**
600	300	1200	0.90	2.52	2.91	3.51	2.91	**1.891**
600	600	300	0.58	1.51	1.56	3.06	1.56	**1.186**
600	600	600	0.76	2.00	2.14	3.42	2.14	**1.530**
600	600	900	0.92	2.55	2.83	3.65	2.83	**1.893**
600	600	1200	0.85	2.41	2.78	2.97	2.78	**1.766**
600	900	300	0.75	1.96	2.03	3.39	2.02	**1.484**
600	900	600	0.92	2.53	2.72	3.70	2.72	**1.867**
600	900	900	0.92	2.62	2.91	3.24	2.91	**1.891**
600	900	1200	0.68	1.91	2.21	2.16	2.21	**1.386**
600	1200	300	0.92	2.52	2.60	3.71	2.60	**1.833**
600	1200	600	0.97	2.75	2.95	3.46	2.95	**1.963**
600	1200	900	0.75	2.13	2.37	2.39	2.37	**1.517**
600	1200	1200	0.52	1.47	1.71	1.68	1.71	**1.073**

This effectively changes the equivalent resistive and inductive components of the feeder frequency response; that is, series or parallel resonances which previously existed may be shifted to either higher or lower frequencies or not exist at all.

In the next case, linear load directly connected at bus 55 provides an alternative path to ground for the harmonic current injection; however, not necessarily a low impedance path. Since this path is now removed, the harmonic currents only path is into the high-voltage system through the distribution transformer; this results in the increased distortion from nominal at bus 55. Although the transformer leakage inductance appearing in series has a smoothing effect, the harmonic currents still propagate along the feeder resulting in increased harmonic voltage drops and distortion.

Table 4 Feeder voltage total harmonic distortion as a function of case loadings.

BUS	*Base Case THD (%)*	*Impedance of C433 lines doubled*	*No linear load at Bus 55*	*No linear load in C433*	*No linear load in DS1*
SSHV	0.02	0.01	0.02	0.02	0.05
SSLV	0.38	0.36	0.40	0.58	1.15
1	0.76	0.85	0.80	1.09	1.66
2	1.01	1.16	1.06	1.42	2.00
3	1.13	1.28	1.19	1.58	2.16
4	1.69	1.87	1.78	2.33	2.92
5	2.00	2.18	2.10	2.73	3.32
6	2.14	2.53	2.25	2.93	3.56
7	2.14	2.52	2.25	2.93	3.56
8	2.14	2.52	2.25	2.93	3.56
55	3.42	2.28	3.57	4.18	4.66
FOM	**1.53**	**1.60**	**1.61**	**2.06**	**2.60**

The results corresponding to the final two cases — no linear load connected to Circuit C433 and DS1, respectively — are consistent with the expected changes in the FOM indice. Since the shunt paths to ground no longer exist and since there is a net decrease in the number and effect of system damping components, then the FOM should increase by an amount which can only be conveniently determined through simulation.

Figure 10 displays the voltage total harmonic distortion versus bus number as a function of loading on Circuit C433. The top and bottom traces represent the no-load and peak-loading conditions, respectively. It can be seen that these traces form an upper and lower bound on the voltage THD existing on the feeder for the assumptions used in this study. Furthermore, this distortion is only attributed to the 11 VSHPs located at bus 55.

Table 5 shows the feeder voltage total harmonic distortion as a function of the distribution transformer (DT) X/R ratio. As seen by the second column in Table 5, the distribution transformer located at bus 55 has a X/R ratio of 1.3. By holding the leakage reactance constant, the resistance is varied to obtain ratios from 0.5 to 15. The FOM indice in Table 5 shows little variation among the different cases.

Figure 10 - Voltage total harmonic distortion versus bus number as a function of loading on Circuit C433.

In fact, the voltage THD upstream from bus 5 (i.e., toward the substation) is relatively constant. The most remote buses in the feeder do show noticeable deviations from nominal — especially at bus 55 — where the harmonic distortion decreases for transformers having higher X/R ratios; these high X/R ratio transformers operate as a harmonic filtering "choke".

Finally, Table 6 displays the feeder voltage total harmonic distortion as a function of the power transformer (PT) X/R ratio. It appears that the PT X/R ratio has a negligible effect on the resulting voltage total harmonic distortion along Circuit C433.

Table 5 Feeder C433 voltage total harmonic distortion as a function of the distribution transformer X/R ratio.

BUS	*DT X/R = 0.5*	*DT X/R = 1.3 Base Case*	*DT X/R = 5*	*DT X/R = 10*	*DT X/R = 15*
SSHV	0.02	0.02	0.02	0.02	0.02
SSLV	0.37	0.38	0.38	0.34	0.38
1	0.74	0.76	0.77	0.77	0.77
2	0.99	1.01	1.02	1.02	1.02
3	1.11	1.13	1.14	1.14	1.14
4	1.66	1.69	1.71	1.71	1.71
5	1.96	2.00	2.01	2.02	2.02
6	2.10	2.14	2.16	2.16	2.16
7	2.10	2.14	2.16	2.16	2.16
8	2.10	2.14	2.16	2.16	2.16
55	3.98	3.42	3.22	3.18	3.17
FOM	**1.56**	**1.53**	**1.52**	**1.52**	**1.52**

Table 6 Feeder C433 voltage total harmonic distortion as a function of the power transformer X/R ratio.

BUS	*PT X/R = 5*	*PT X/R = 10*	*PT X/R = 14.4 Base Case*	*PT X/R = 20*	*PT X/R = 25*
SSHV	0.01	0.02	0.02	0.02	0.02
SSLV	0.33	0.37	0.38	0.39	0.39
1	0.71	0.75	0.76	0.77	0.77
2	0.96	1.00	1.01	1.02	1.02
3	1.08	1.12	1.13	1.14	1.14
4	1.64	1.68	1.69	1.70	1.71
5	1.94	1.98	2.00	2.01	2.01
6	2.08	2.12	2.14	2.15	2.16
7	2.08	2.12	2.14	2.15	2.15
8	2.08	2.12	2.14	2.15	2.15
55	3.37	3.41	3.42	3.43	3.43
FOM	1.48	1.52	1.53	1.54	1.54

References

[1] Electrotek Concepts, *Power Quality Assessment Procedure*, EPRI Report CU-7529, Project 2935-13, December 1991.

[2] J. Arrillaga, D. A. Bradley, P. S. Bodger, *Power Systems Harmonics*, John Wiley & Sons, New York, NY, 1989.

[3] J. C. Balda, K. J. Olejniczak, R. Tirumala, M. J. Samotyj, B. Barbr, "A Study of Voltage Distortion Caused by Variable Speed High-Efficiency Heat Pumps", *Proceedings of the IEEE-IAS 1993 Annual Meeting*, pp. 1579-1585, Toronto, Canada, October 2-8, 1993.

Kraig J. Olejniczak
Prof. Juan Balda
Department of Electrical Engineering
University of Arkansas

Harmonic Filters

Specifying Harmonic Filters for Industrial Applications

Although industrial 480 V and 4.16 kV harmonic filters are customized equipment, they are treated as a commodity in the marketplace. Competing mostly on price, manufacturers are forced to provide what the buyer demands, and no more. Therefore, the customer must determine the minimum requirements for a satisfactory design. This article describes some of these considerations, and provides a list of filter vendors covering the North American market.

Overload Protection

Fuses can protect filters from high fault currents, but may not be effective in preventing a failure due to overload. This is a serious problem, because the potential for unanticipated harmonic currents is high. Common causes are:

- Filter design based on an analysis that underestimated harmonic load, or on measurements that did not capture the worst-case harmonic injection.
- Nonlinear load in the facility eventually grows to the point of overloading the filter.
- Filter draws unexpectedly high harmonic currents from sources outside the plant.

Minimizing the potential for overload requires a conservative filter design. It is good practice to run two simulations, one using the worst-case harmonic injection to check THD, TDD at the point of common coupling, etc., and one using the worst-case injection multiplied by some safety factor to check filter duties. Be sure to account for distortion in the utility supply voltage - assuming the maximum allowed by IEEE-519 is a conservative assumption if measurements are not available.

The reactor current spectrum from the second simulation should be included in the specification document. The specification should require that when the reactor carries this current spectrum, the temperature rise should not exceed

50% - 90% of the maximum allowable temperature rise for the insulation system used. (The exact percentage depends on how conservative you wish to be.) If the filter consists of multiple steps switched in and out by an automatic controller, include a short-time overload requirement to account for lag in controller response when the load is suddenly increased, e.g., "the temperature rise shall not exceed the maximum allowable when the reactor carries twice the maximum expected harmonic currents for a period of 45 seconds."

Finally, some means should be provided for tripping the filter if an overload does occur. For low voltage filters, this can be done by using thermal sensors imbedded in the reactor windings to provide a trip signal to the filter contactor. Imbedded sensors may limit BIL in medium voltage reactors. If this is a concern, the filter breaker or contactor can be tripped via a thermal overload relay.

Unbalance Detection

4.16 kV filters commonly employ individually-fused capacitors connected in parallel. One blown fuse will shift the filter tuning, increasing the current in the remaining capacitors, and possibly leading to a cascade of fuse operations before the filter overload protection can trip. Therefore, medium voltage filters should normally have some form of unbalance detection.

Low voltage filters often do not employ individual fuses for parallelled capacitors, a consequence of their metallized paper or metallizied polypropelene construction. A dielectric failure causes the thin metal film around the fault point to vaporize, producing a low magnitude, self-clearing fault. Repeated dielectric failures will generate sufficient gas to cause a pressure-activated switch to de-energize the capacitor.

Whether by fuses or pressure switches, if individual capacitors can be de-energized, the bank should be tripped. However, the fact is that many customers are not willing to bear the additional cost of unbalance protection for a low voltage filter, especially if the reactors have thermal overload protection. Vendors that do provide unbalance protection have found these methods to be the most economical:

- Trip the bank contactor via a signal from auxiliary contacts on the capacitor pressure switches.
- Use a single capacitor in each leg of the delta. This eliminates the major concern of damage to parallel units. There is still the possibility of

overcurrents in capacitors in the other legs, but the loss of one unit will probably shift tuning so much that this will not be the case.

Iron Core vs. Air Core Reactors

Air core reactors are larger and usually - though not always - more expensive than iron core. However, high reactor current during fault or unbalance may saturate an iron core, causing reactor inductance to decrease to the value that an air core reactor of the same winding geometry would have. This further increases the current, and the resulting mechanical forces on the windings may cause damage before the fault can be cleared by the filter overcurrent protective device.

Reactor damage can be prevented by improving the core saturation characteristic (amount of iron, air gap dimensions), employing current-limiting fuses, or enhancing the ability of the winding to withstand the mechanical forces. It is rarely necessary to resort to an air core design for 4.16 kV and 480 V filters.

The filter specification document should include the fault duty at the filter bus, together with language requiring that the reactors be protected from capacitor faults. Specifying some minimum saturation level, on the other hand, means little because no standard testing procedure has yet been established.

Component Tolerances

Capacitor standards require that actual capacitance fall within -0% to +15% of rated. Reactor standards don’t define a tolerance for inductance, but ±2.5% or ±5.0% of nameplate commonly appears on filter specifications.

Capacitor manufacturers usually impose much tighter tolerance bands on their products. For example, units from one manufacturer invariably fall within +6% to +8% of rated, while units from another manufacturer range from +2% to +4%.

Most filter vendors build their own reactors, but purchase capacitors “off the shelf.” Thus, they can accommodate a specification that imposes a limit on reactor tolerance, but may not be able to do so (at least, not without changing suppliers) if a limit is imposed on capacitor tolerance.

The reason that limits are placed on capacitor and reactor tolerance is to control filter tuning. Therefore, it makes more sense to specify a tuning tolerance directly, e.g., 282 - 288 Hz. It should be stipulated that the filter will achieve the required tuning when energized at rated current, as tuned frequency tends to decrease at high current due to flux fringing effect in the reactor.

It should be further stipulated that the tuning in all three phases must fall within the required tolerance. The purpose of this requirement is to limit impedance unbalance, which is inherent in three-phase reactor designs due to unsymmetric mutual coupling. This is not a concern when single-phase reactors are used.

Reactor Insulation Levels

Voltage withstand requirements for reactors are not yet defined in industry standards. Some manufacturers use the *IEEE Standard General Requirements for Dry-type Distribution and Power Transformers* (ANSI/IEEE C57.12.01) as a guideline for reactor BIL and low frequency ("hi-pot") withstand. Other manufacturers provide a BIL consistent with the *IEEE Standard for Shunt Power Capacitors* (IEEE Std. 18).

C57.12.01 BIL should be adequate for a filter applied indoors with an arrester-protected service entrance transformer between the filter and overhead distribution lines. The filter bus should be protected by a surge suppresser that coordinates with the reactor BIL. The higher BIL requirements of IEEE Std. 18 are justified for outdoor or other locations with a high exposure to impulse transients.

	kV	
Test	**480 V**	**4.16 kV**
C57.12.01 Low Frequency	4	12
C57.12.01 BIL	10	30
IEEE Std. 18 BIL	30	75

Table 1. Voltage withstand requirements for capacitors and dry-type transformers.

Standard Capacitor Tests

The specification document should require that the filter capacitors have a UL or CSA rating and meet the testing requirements contained in the following standards:

- IEEE Std 18: RMS and peak kV, RMS current, RMS kvar.

- NEMA Standard C1 5.10-5.12: short time overload, capacitance, loss determination, discharge resistor, leak, impulse, bushing, radio influence voltage, voltage decay.

Are Over-Rated Capacitors Necessary?

An article in a previous issue of the *Resonant* described why fundamental voltage will rise across a filter reactor, increasing RMS voltage on the capacitor. The lower the filter tuning, the higher the capacitor overvoltage will be. For example, a fifth harmonic filter tuned at 282 Hz will have a fundamental capacitor voltage 4.7% higher than bus voltage. After adding an allowance for normal variations in utility supply voltage - ANSI C84.1 allows a "range B" (short-time) limit of +5.8% - it can be seen that capacitor RMS voltage can exceed 110% limit specified by IEEE Capacitor Std. 18 even with no harmonic loading.

One solution would be to use custom-built capacitors rated at 110% of nominal bus voltage, but with one or two exceptions, vendors employ off-the-shelf units: 600 V rating at 480 V, and 4.8 kV rating at 4.16 kV. Unfortunately, the kvar delivered by the capacitor drops off with the square of the ratio of applied voltage to rated voltage - the 600 V capacitor will deliver only 64% of rated kvar, and the 4.8 kV capacitor will deliver only 75%. If the filter must provide power factor correction, capacitor size (and cost) must be increased accordingly.

When induction motors comprise most of the load in a facility, the rationale for installing filters is to provide power factor correction without creating a resonance, rather than to reduce distortion levels. The filters do not need to absorb large amounts of harmonic amperes in order for the plant to meet IEEE-519 guidelines, so they are not tuned very close to their target harmonic frequencies. In this scenario, it may not be necessary to increase capacitor voltage rating for a fifth-harmonic filter, because the rise in RMS voltage due to harmonics may be offset by a drop in fundamental voltage due to heavy motor load.

If capacitors rated at nominal voltage are used in a fifth-harmonic filter, the service transformer taps should be adjusted to prevent excessive voltage rise at low load. This may not be necessary if the filter is switched off at low load by an automatic power factor controller. As illustrated in Figure 1, when load kvar has increased to the level that causes the first step to switch on, the load kW may have reduced fundamental voltage sufficiently.

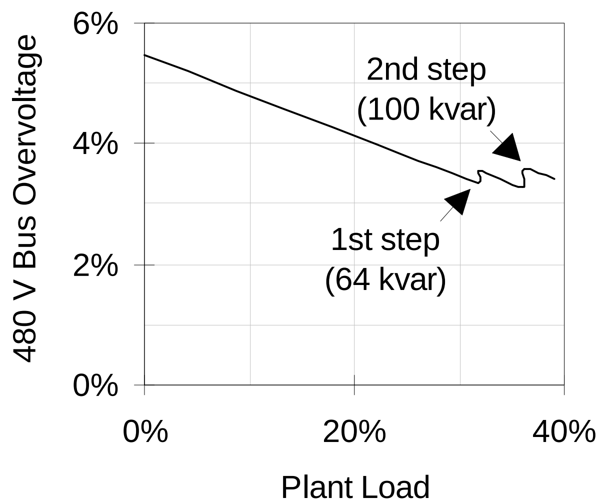

Figure 1. Effect of plant loading and energizing filter steps steps on bus voltage.

Before capacitors rated at nominal voltage are considered, sufficient measurements should be conducted to precisely characterize variations in harmonic loading and bus voltage. Specify over-rated capacitors if there is any doubt.

Rory Dwyer
Senior Power Systems Engineer
Electrotek Concepts, Inc.

Filter Vendors

ABB (≤ 600 V)
Steve Colvin
1206 Hatton Road
Wichita Falls, TX 76302
817-761-3232 / 817-761-3202

Aerovox Group
John Childs
740 Belleville Ave.
New Bedford, MA 02745-6194
508-994-9661 / 508-990-8696

ASC Industrial
Bruce Marzley / Larry Burch / Chuck Gougler
8967 Pleasantwood Ave NW
North Canton, OH 44720
216-499-1210 / 216-499-1213

Commonwealth Sprague (≤ 600 V)
Frank Smith
Brown Street
North Adams, MA 01247
413-664-4466 / 413-664-4465

Controllix
Paul Griesmer
21415 Alexander Road
Walton Hills, OH 44146
216-232-8757 / 216-232-1893/

Freeborn Industries
Rudy Wodrich / Kevin Simpson
6675 Rexwood Road
Mississauga, Ontario
L4V 1V1 Canada
905-677-9272 / 905-677-5448
can also contact any Square D office, or Schneider Canada at above address


Member HUG

General Electric
Peter Baltz
14131 Midway Road, Suite 500
Dallas, TX 75244
214-702-5274 / 214-702-5283

Gilbert/K&M Electrical Systems & Products
Neal Ciurro / Jess Hancock
P.O. Box 1141
Beckly, WV 25802
304-252-6243 / 304-252-6292

Macroamp Lesat
Bob Stuefen / Allan Freebury
P.O. 1512
Ukiah, CA 95482
707-462-2222 / 707-462-3068

Myron Zucker (≤ 600 V)
Jim Holley
315 East Parent Street
Royal Oak, MI 48067
810-543-2277 / 810-543-1529

Robicon
Dennis Lorenzi
100 Sagamore Hill Road
Pittsburgh, PA 15239-2982
412-325-7260 / 412-733-8093

Shallbetter (≥ 2.4 kV)
Doug Johnson
640 Arizona Ave. NW
Huron, SD 57350
605-352-1559 / 605-352-5562

TCI (≤ 600 V)
J. P. Thorpe
7878 North 86th St.
Milwaukee, WI 53224
414-357-4480 / 414-357-4480

Tech-Tran Corp
Ted Furst / Charles Roney
50 Indel Avenue
Rancocas, NJ 08703
800-257-9420 / 609-267-6751

VAR+ Controls
Bill McConnell / Brian Prokuda
Mail Box 585
Whitmore Lake, MI 48189
800-KILOVAR / 313-449-8710


Member HUG

Versatex Industries (≤ 600 V)
Ted Noutko
P.O. Box 354
Brighton, MI 48116
810-229-5751 / 810-229-7863